

**CONSTITUTIVE MODELING OF THE STRESS-
SOFTENING IN SWOLLEN
POLYCHLOROPRENE RUBBER UNDER
CYCLIC LOADING**

RAIHANA BINTI MOHAMAD FAWZI

**RESEARCH REPORT SUBMITTED IN PARTIAL
FULFILMENT OF THE
REQUIREMENTS FOR THE DEGREE OF MASTER OF
ENGINEERING**

**FACULTY OF ENGINEERING
UNIVERSITY OF MALAYA
KUALA LUMPUR
2012**

ABSTRACT

Research and development of alternative source to substitute fossil fuel are getting demanding since fossil fuels are non renewable. Thus energy insecurity becomes a critical issue. Biodiesel is one of the alternatives explored for the substitution. However, the compatibility of biodiesel with the elastomeric components such as o-rings and seals is still questionable. In practical engineering application, the materials are subjected to hostile liquid such as biodiesel which leads to swelling and is also subjected to fluctuating or cyclic mechanical loading which could lead to fatigue failure. Similarly to dry elastomer, swollen elastomer exhibit inelastic response under cyclic loading such as stress softening, hysteresis and permanent set. These inelastic responses play major role on the durability of the materials. In the present work, a simple continuum model to capture the stress softening of swollen polychloroprene is addressed. The stress softening in swollen elastomer is considered as a damage process. Thus it is described phenomenologically by a scalar quantity which depends on the swelling level and the maximum strain experienced by the materials. Moreover, the first invariant of the left Cauchy-Green Strain tensor is adopted as the scalar strain measure. The results obtained show a qualitatively good agreement between the model and experiment.

ABSTRAK

Penyelidikan dan pembangunan sumber alternatif untuk menggantikan bahan api fosil semakin mendesak disebabkan bahan api fosil adalah sumber yang tidak boleh diperbaharui. Biodiesel adalah salah satu alternatif yang diterokai untuk tujuan penggantian. Walau bagaimanapun, keserasian biodiesel dengan komponen elastomer masih boleh dipersoalkan. Dalam aplikasi kejuruteraan praktikal, bahan-bahan tersebut terdedah kepada cecair seperti biodiesel yang boleh mengakibatkan pembengkakan apabila tertakluk kepada beban yang berubah-ubah atau kitaran mekanikal yang boleh membawa kepada kegagalan. Ini memainkan peranan utama pada ketahanan bahan-bahan. Dalam kajian ini, satu model kontinum mudah menunjukkan kesan pembengkakan apabila polychloroprene terdedah kepada cecair biodiesel dikaji. Tekanan dalam elastomer bengkak dianggap sebagai proses kerosakan. Oleh itu, digambarkan fenomenologi sebagai kuantiti skalar yang bergantung kepada tahap bengkak dan terikan maksimum yang dialami oleh bahan-bahan. Tambahan pula, tensor terikan kiri Cauchy-Green diguna pakai sebagai langkah terikan skalar. Hasil yang diperolehi menunjukkan hasil yang baik antara model dan eksperimen.

ACKNOWLEDGEMENT

First and foremost, I would like to thank my supervisor of this project, Dr. Sr Andri Andriyana for valuable guidance and advice. He inspired me greatly to work in this project. His willingness to give a motivation contributed tremendously to this project.

Besides that, an honorable mention goes to my families and friends for their patience, understandings and supports on completing this project. Without help of the particular that mentioned above I would probably face many difficulties while doing this project.

TABLE OF CONTENTS

Declaration Letter	
Abstract (English)	ii
Abstract (Malay)	iii
Acknowledgement	vi
Table of Contents	v
List of Figure	vii
List of Table	ix
Nomenclatures	x
Chapter 1 Introduction	1
1.1 Background	1
1.2 Problem Statement	5
1.3 Objective	6
Chapter 2 Literature Review	7
2.1 Biodiesel	7
2.2 Elastomers	13
2.3 Polychloroprene (CR)	15

	2.4 Stress Softening	17
	2.5 Mechanical behavior of elastomer in biodiesel	19
Chapter 3	Methodology	22
Chapter 4	Result and Discussion	26
	4.1 Development of equations, determination of material parameters and comparisons	26
	4.1.1 Development of equations	26
	4.1.2 Material constant determination	31
	4.1.3 Comparison model with experimental result	34
	4.2 Modeling with the First Invariant	35
	4.3 Discussion	40
Chapter 5	Conclusion and Recommendations	44
	5.1 Conclusion	44
	5.2 Recommendations	45
	Bibliography	

LIST OF FIGURES

1. Figure 2.1: Transesterification of triglycerides (TG) from plant and animal fats in presence of a base catalyst is the traditional route to produce biodiesel
2. Figure 2.2: Stress strain curve of elastomer
3. Figure 2.3: Hysteresis exhibited by elastomers
4. Figure 2.4: Stress relaxation of elastomers
5. Figure 2.5: Stress relaxation of elastomers
6. Figure 2.6: Microscopic description of Stress Softening Effect
7. Figure 2.7: Filler particle–chain junctions
8. Figure 4.1: Experimental Stress Ratio
9. Figure 4.2: Experimental Stress Softening for dry rubber
10. Figure 4.3: Experimental Ratio of Stress Softening
11. Figure 4.4: Stress at first uploading for dry rubber
12. Figure 4.5: Stress Ratio of experimental and model
13. Figure 4.6: Experimental and theoretical stress softening curve for the dry rubber
14. Figure 4.7: The experimental and theoretical curve for ratio of the stress softening
15. Figure 4.8: Stress at first uploading

16. Figure 4.9: Stress at second uploading
17. Figure 4.10: Stress Ratio as a function of I_1
18. Figure 4.11: Stress Softening as a function of I_1
19. Figure 4.12: Ratio of Stress Softening as a function of I_1
20. Figure 4.13: Stress at first uploading as a function of I_1
21. Figure 4.14: Stress at second uploading as a function of I_1
22. Figure 4.15: Theoretical stress at first and second uploading
23. Figure 4.16: Stress softening of swollen rubber compared to dry rubber

LIST OF TABLES

1. Table 2.1: Oil productivity of major oil crops
2. Table 2.2: ASTM requirement of biodiesel
3. Table 2.3: Emmision of biodiesel
4. Table 4.1: The value of material constant
5. Table 4.2: Summary of material constant value in 8-chain model

NOMENCLATURES

σ	Tensor Stress
ε	Strain
λ	Principle Stretch
β	Swelling
V_2	Volume Rubber Fraction
V_{2eq}	Equilibrium condition of volume fraction
W_o	Undamaged strain energy function
d	Damage parameter
p	Lagrange multiplier
I_1	First stress invariant
I_2	Second stress invariant
\mathbf{B}	Left Cauchy-Green
σ^{1up}	Stress at first uploading
σ^{2up}	Stress at second uploading
SR^*	Stress Ratio
SS	Stress Softening
RSS	Ratio of Stress Softening

CHAPTER 1: INTRODUCTION

1.1 General Introduction

Presently, coal, oil and natural gas which are referred as fossil fuels are world's main supply of energy. These fossil fuel are said to be non-renewable due to the rate at which they are generated is very much less compared to the rate they are depleted. Petroleum oil takes millions year to form (Demirbas, 2008).

According to The American Petroleum Institute, it is estimated in 1999 that the world's oil supply would be depleted in between 2062 to 2094. This is assuming that the world's oil reserve is between 1.4 and 2 trillion barrels and the consumption is estimated 80 million barrel per day. However, a study in 2004 showed that the world's reserve of petroleum oil to be 1.25 trillion and the consumption per day is 85 million barrels. This recent study shifted the estimated depletion of oil at 2057. (Geiver, 2011)

Besides being a non renewable source of energy, petroleum oil has quite a big impact to our environment. The burning of oil in automobiles raises the level the carbon dioxide in the atmosphere. This extra emission of carbon dioxide gasses causes the earth to be warmer than it is supposed to be. Besides that, petroleum oil contains sulfur which produces sulfur dioxide when burnt. These compounds form surfuric acid which leads to acid rains when combined with the atmospheric moisture. Acid rains causes acidification of the lakes and stream and also destruction of forest. Acid rain also causes the acceleration of the decay of

paints, building materials including irreplaceable buildings, sculptures and statues that are part of nation's heritage (Mohammed, 2011).

The transportation of oil also could cause negative impact to the environment. The most common transportation means of petroleum is through sea by supertanker. Although, oil spillage is a rare issue, once occurred it causes big disaster to the marine life, birds and the coast for a long period of time. Petroleum oils contain chains of hydrocarbon. The bond degrading of this hydrocarbon bond are greatly facilitated by the high content of nitrogen and phosphorus which are limited in sea water. This causes the degradation of the petroleum consumes long period of time (Shigeaki, Hideo, Yuki, & Kazuaki, 1999).

Moreover, majority of countries where oil can be found has unstable political situation. Most of the world's oil reserve which is believed 70 percent at Middle East countries are facing unstable political conditions. Oil dependent developed nations may influence the politics of the oil reserve countries and take it to their advantage. Riots and instability within the countries could also occur due to this oil reserve. For example in Indonesia, the Aceh Freedom Movement criticized the government for stealing the oil situated at Aceh and using this issue as the reason for separation. They also claimed that they could be as rich as Brunei if it is declared as a free country (Karl, 2007).

Due to the issues discussed above and many more, there has come a need to find or develop an alternative for petroleum that could partially solve the issues

and at the same time provide equivalent performance as the commercial petroleum.

Biodiesel is fatty acid methyl esters that are prepared from any type of feedstock which includes vegetable oils, animal fats, single cell oils, and waste material. Biodiesel is produced by the method of transesterification of animal fats or vegetable oil with alcohol usually methanol where catalyst normally sodium methoxide is present. Biodiesel can be produced by many types of feedstock materials such as soybeans, olive oils, sunflower, hazelnuts and the primary is oil palm (Demirbas, Progress and recent trends in biodiesel fuels, 2009).

The major advantage of biodiesel is the fact that it is made from renewable sources. These sources to produce biodiesel oil are easily available. Also, the rate of the generation of the feedstock to produce biodiesel is high and comparative to the rate they deplete (Geiver, 2011).

In environmental aspect, biodiesel is a better choice due to the sulphur emission of biodiesel burning is much lesser compared to commercial petroleum. Although biodiesel burning produces carbon dioxide emission, it will be absorbed by the crops that were grown to make the biodiesel. This emission of carbon dioxide does not contribute to global warming. Since biodiesel are made of organic feedstock it is much more biodegradable and easily degrades if there is any spillage during the transportation (Mohammed, 2011).

However, biodiesel has some disadvantages. One of the disadvantages is the production of biodiesel uses mainly feedstock that are meant as food. This could lead to situation of food deprivation. Some third world countries with high production of biodiesel source will tend to give importance of exporting feedstock such as corns, soya beans and many more to strengthen their economic situation. This excessive export of this feedstock may result insufficient food available for the people.

Besides that, biodiesel is very prone to be contaminated by water which could lead to corrosion, rotten filters, pitting in the piston and many more. Moreover, they may be degradation in the parts of the engine upon exposure to biodiesel for a long time (Hansen, Qin, & Robert, 2009). In an automobile engine fuel system, there are a lot of parts or components made either from metal (ferrous and non-ferrous alloy) and elastomer which directly in contact with the fuel. These materials will interact chemically with the fuel. The interaction of biodiesel is different compared to the conventional petroleum diesel. It can cause corrosive and tribological attack on metallic components and degrade elastomer parts rapidly. Few researches have been done to present an overview of the work done so far on the compatibility of biodiesel with automotive materials.

In case of elastomeric component, a lot of study has been done to see the compatibility of this material in contact with biodiesel. One of them is Haseeb et al, 2010 which study the compatibility of elastomer in palm biodiesel. When the elastomer is in contact with fuel, it will change chemically and physically. The changing is depending on the ability of the material to absorb the fuel or being

dissolved by the fuel. It will also affect the physical characteristic of the material including swelling, shrinkage, embrittlement and changes in tensile properties.

Under static mechanical loading for example, the material that swell in the fuel will suffer from a hardness problem but still can be continually use for a long time. However, in dynamic applications, the swelling may give more serious effect. It will increase the friction and wear and finally impact the engine durability. Thus, it is necessary to understand the effect of contamination on mechanical performance and durability of the elastomer in biodiesel.

1.2 Problem Statement

Under cyclic loading, swollen rubber exhibits inelastic response such as hysteresis, stress softening and permanent set. The current study and modeling of the above responses is essential for the durability of the material. Many models that are available in the literature focus on the study the inelastic response in dry elastomer whereas there are no studies conducted in swollen elastomers. Thus, it is essential to develop a model that investigates the behavior of swollen elastomers exposed to cyclic loading.

1.3 Objectives of Study

The objectives of the study are listed as below:

1. To develop a simple continuum mechanical model to capture stress-softening effect in swollen polychloroprene (CR) under cyclic loading
2. To compare the result of the model and the experimental observation

CHAPTER 2: LITERATURE REVIEW

2.1 Biodiesel

Transportations mostly dependent on fossil fuels particularly petroleum based. The dependency on petroleum fuel creates a danger because of its non-renewable energy nature as well as many other reasons such as environmental impact, political security impact, finance impact and many more. These reasons serve as a solid argument why there is a need to explore and develop alternative source for fuel especially for transportation needs.

Currently, research on biofuel as an alternative source for fossil fuel is widely conducted. Biodiesel are energy sources which are renewable produced from natural biobased material. Examples of common biofuels are ethanol from corn, wheat or sugar beet and biodiesel from oil seeds (Demirbas, 2008).

Biodiesel is associated to a vegetable oil or animal fat based diesel fuel containing a long chain of alkyl esters. Biodiesel feedstocks include virgin oil, waste vegetable oil and animal fat. Examples of virgin oils are mustard, flax, palm, hemp, Jatropha and sunflower. Waste vegetable oil is oils that have been discarded after use such as canola oil. Tallow, lard, yellow grease, chicken fat, and the byproducts of Omega 3 fatty acids from fish oils are example of animal fats.

One of most popular source for biodiesel production is from palm oil. One third of global comes from palm oil. This is due to its high annual yield per hector compared to other source of oilseeds. As shown in Table 1, the average annual

yields for palm biodiesel 3.88 tons per hacter. Other source such as soybean only used 0.36 tons/ha. This is one of the reason why palm oil is one of the major source of feedstock for biodiesel (Basiron, 2007).

Table 2.1: Oil productivity of major oil crops. (Basiron, 2007)

Oil crop	Oil production [million tonnes]	% of total production	Average oil yield [tonnes/ha/year]	Planted area [million ha]	% of total area
Soyabean	33.58	31.69	0.36	92.10	42.24
Sunflower	9.66	9.12	0.42	22.90	10.50
Rapeseed	16.21	15.30	0.59	27.30	12.52
Oil palm	33.73	31.84	3.68	9.17	4.21
Total [§]	105.94			218.02	

The current technology production method of biodiesel is by homogeneous catalytic of triglycerides in the feedstock which is known as transesterification. This reaction is normally conducted at ambient pressure and temperature of 40°C. The stoichiometry of the reaction is as figure below. In this reaction 3 molecules of alcohol that is methanol is reacted with one molecule of triglycerides to produce three molecules of fatty acid methyl ester which is biodiesel and one molecule of glycerol (Gerpen, 2006).

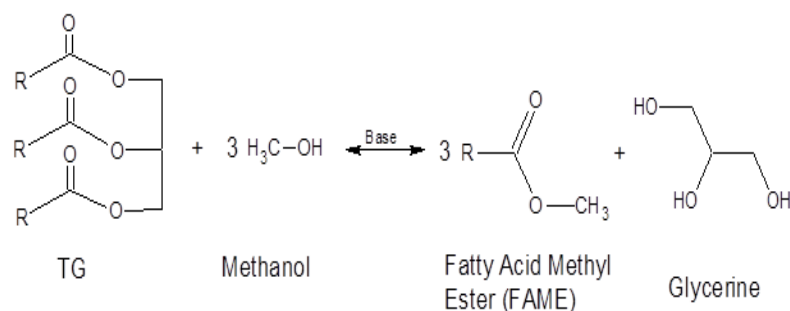


Figure 2.1: Transesterification of triglycerides (TG) from plant and animal fats in presence of a base catalyst is the traditional route to produce biodiesel (Gerpen, 2006).

Table 2 below show the comparisons between property of biodiesel and convention diesel. Biodiesel is known to have high cetane number that will cause easy ignition and produce less noise. The viscosity of biodiesel is low after transesterification. High viscosity will cause poor atomization of the fuel spray and make the operation of fuel injector less effective. The low viscosity of biodiesel makes it easier to pump and atomize and produce fine droplets (MN & Beg, 2004).

Table 2.2: ASTM requirement of biodiesel (Crimson Renewable Energy, 2007)

Fuel Property	Diesel	Biodiesel	Units
Fuel Standard	ASTM D975	ASTM D6751	
Lower Heating Value	~129,050	~118,170	Btu/gal
Kinematic Viscosity @ 40° C	1.3 - 4.1	1.9 - 6.0	mm ² /s
Specific Gravity @ 60° C	0.85	0.88	kg/l
Density	7.079	7.328	lb/gal
Water and Sediment	0.05 max	0.05 max	% volume
Carbon	87	77	wt. %
Hydrogen	13	12	wt. %
Oxygen	0	11	
Sulfur	0.0015	0.0 to 0.0024	wt. %
Boiling Point	180 to 340	315 to 350	° C
Flash Point	60 to 80	130 to 170	° C
Cloud Point	-15 to 5	-3 to 12	° C
Pour Point	-35 to -15	-15 to 10	° C
Cetane Number	40 to 55	47 to 65	
Lubricity SLBOCLE	2,000 to 5,000	>7,000	grams
Lubricity HFRR	300 to 600	<300	microns

The most prominent advantage of biodiesel is that it is a renewable energy source. The source or feedstock used to produce biodiesel oil are easily producible and does not deplete (Demirbas, 2008).

Another advantage of biodiesel is in environmental aspect. This is because biodiesel burns clean diesel fuel that gives minimum negative impact to the environment and helps to reduce the emission of green house gas. Biodiesel production and utilization when compared to petroleum diesel, produces 78.5 percent less CO₂ emissions. Carbon dioxide is consumed by the annual production of crops and then released when vegetable oil based biodiesel is combusted. Moreover, pure biodiesel is has no content of sulfur and it reduces the emission of sulfur dioxide as well as sulfur aerosols (Mohammed, 2011).

Table 2.3: Emission of biodiesel (Mohammed, 2011).

Emission Type	B100	B20
Regulated		
Total Unburned Hydrocarbons	-67%	-20%
Carbon Monoxide	-48%	-12%
Particulate Matter	-47%	-12%
NO _x	+10%	+2% to -2%
Non-regulated		
Sulfates	-100%	-20%*
PAHs (Polycyclic Aromatic Hydrocarbons)**	-80%	-13%
nPAHs (nitrated PAHs)**	-90%	-50%***
Ozone potential of speciated HC	-50%	-10%

*Estimated from B100

**Average reduction across all compounds measured

***2-nitrofluorine results were within test method variability

Besides that, biodiesel are rapidly biodegradable and completely non toxic. B100 which is 100 percent content of biodiesel is as biodegradable as sugar and is less toxic than conventional table salt. The rate that biodiesel are biodegradable is almost four times higher that diesel made from fossil fuel. It could be 98 percent biodegradable in three weeks. Thus, spillage of biodiesel during transportation exhibit lower risk compared to fossil fuels (Karl, 2007).

The temperature to which the fuel must be heated to produce a vapor mixture above the surface of the fuel that will ignite when exposed to ignition source such as spark or flame is referred as flash point. This is an important factor for operating fuel in underground mines. It is observed that as the concentration of biodiesel increases its flash point increases. Thus, biodiesel and its blend with petroleum diesel are safer to handle and store compared to fossil (2008).

However, biodiesel fuel also exhibits some disadvantages. One of it is contamination during the process of production, transportation, storage and due to degradation. The most common contamination associated is water which could promote microbial growth. This is because biodiesel is hygroscopic and causes water separation. This contamination causes the biodiesel fuel does not meet the requirement of ASTM (Howell & J.).

The cost of biodiesel is higher than diesel fuel. The cost of biodiesel is higher if compared to diesel fuel. This is because biodiesel production and technology are still new in research and the cheapest method of production is yet to be explored. Besides that, it takes into consideration the cost of land. Thus, to overcome this, cheap source of feedstock should be explored. Also, another drawback of biodiesel is, there is a fear of depletion of food source if most of source of food is used to generate biodiesel fuel (Demirbas, 2008).

Biodiesel has excellent solvent properties compared to petroleum fuel. Thus, any deposits in the filters and in the delivery systems may be dissolved by biodiesel and cause the need for replacement of the filters. This is because biodiesel can loosen those deposits, and they migrate and clog fuel lines and filters (Demirbas, 2009).

Although biodiesel has proven to be able to give similar operating performance if compared to commercial fossil fuel, its compatibility to the other material in engine part partly made of elastomers such as o-rings, seals, belts and others are still questionable. Some incident shows fuel injection pump leak using

biodiesel fuel is due to failure of o ring seals. Biodiesel in contact with these elastomers causes it to swell. This is due to fluid or chemical absorption by elastomer materials lead to swelling. This is due to the aromatic content of the fuel. Elastomers are prone to be attacked by fluids exhibiting the same polarity in a phenomenon described as 'like-dissolves-like'. The polarity of biodiesel increases its solvent intense and fastens the process of permeation. This leads to change in important physical properties of elastomers such as tensile strength, elongation, flexibility, modulus and dimensional change. These changes would promote degradation of materials. As a solution, a proper and suitable blend of biodiesel with diesel should be used. Besides that, it is suggested to use materials that are suitable with biodiesel as parts of engine. Also, some studies could be conducted on determining the time for degradation of existing o-rings and seals material so that a time could be estimated for replacement. (Kerwin, 2007).

2.2 Elastomers

Elastomer is defined as a polymer that can stretch and then return to its original shape without permanent deformation. It exhibits viscoelasticity properties which usually has high yield strain and low Young's modulus. These elastomers are amorphous polymer existing above their glass transition temperature which enables them to have considerable segmental motion. Also, elastomers are only slightly cross-linked.

Elastomers are the raw state of rubber. Rubbers are compounded and vulcanized. This vulcanization process forms chemical bonds between adjacent elastomer chains and eventually imparts dimensional stability, strength and resilience. Rubber exhibits low modulus of elasticity and is able to sustain deformation almost 1000 percent. After being deformed it is able to return to its original dimension. Besides that, it is flexible and is able to be processed and molded into variety shape. It also has high resistance towards corrosion attack and requires no lubrication.

The stress strain curve for an elastomer undergoing tensile is illustrated as figure 2.2 below. After undergoing a large percentage of elongation, the curve becomes non linear. Elastomers has lower modulus elasticity at the initial curve and increases with increasing strain until it fails. Elastomers are generally incompressible where it mostly changes in shape rather than changes in volume.

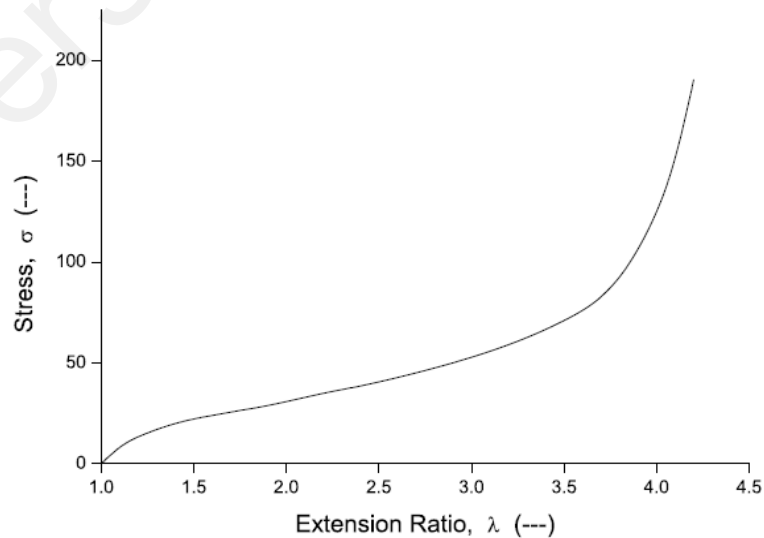


Figure 2.2: Stress strain curve of elastomers. (Bauman, 2006)

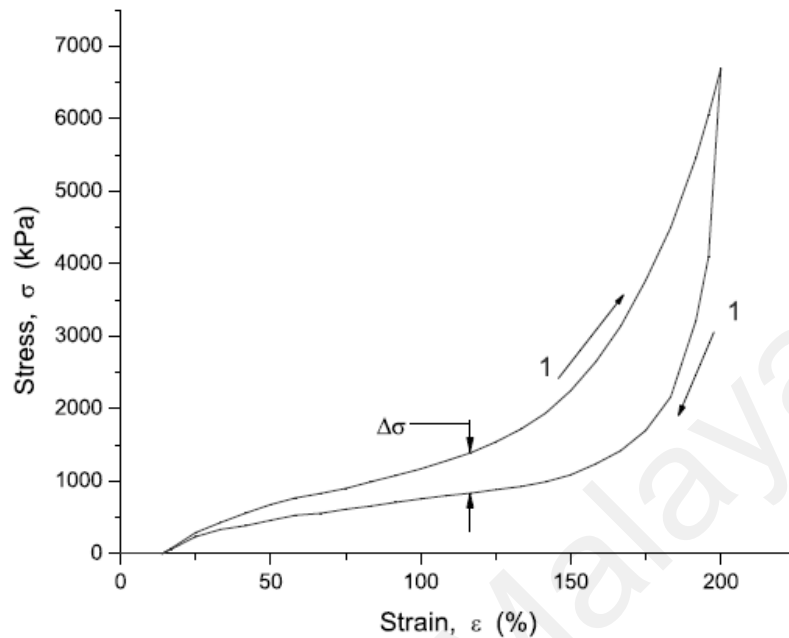


Figure 2.3: Hysteresis exhibited by elastomers. (Bauman, 2006)

Another physical property of elastomer is hysteresis as in figure 2.3. Hysteresis that occurs in elastomers is usually caused by the internal friction which resists the extension and contraction. Hysteresis differs with the type of elastomers. If the elastomers are unreinforced, the hysteresis is less compared to reinforced elastomers where internal friction is high.

In figure 2.4 it could be observed that two successive extension and retraction cycles taken to the same maximum stroke. The decreased measures stress of the second cycle is due to the stress relaxation which is the decrease in stress with time at constant deformation. The stress relaxation occurs in rubber due to the slipping of the entanglements which loosens up the network of molecular chain. This result in less force is applied (Bauman, 2006).

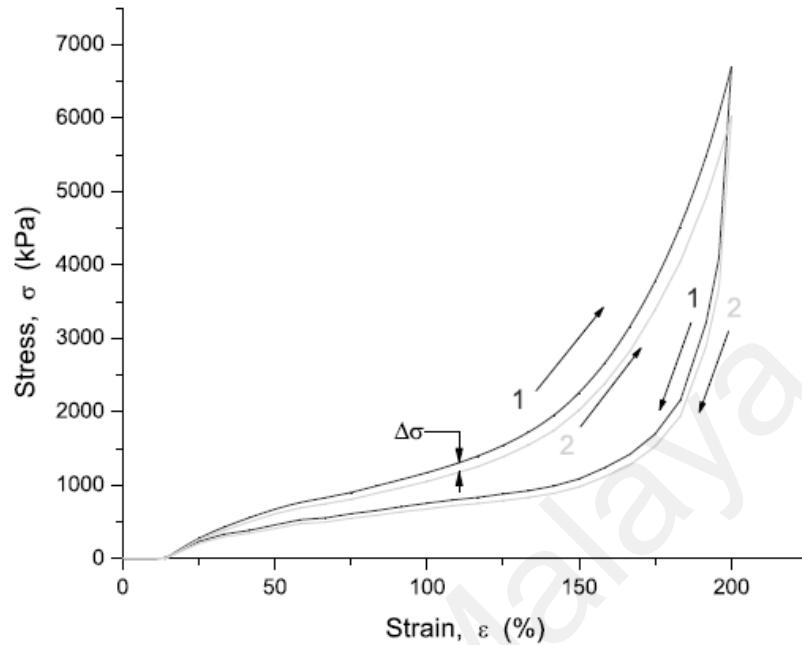


Figure 2.4: Stress relaxation of elastomers (Bauman, 2006)

2.3 Polychloroprene (CR)

One type of elastomer is polychloroprene (CR). Polychloroprene was first produced in 1932 by DuPont and its commercial name is Neoprene.

Polychloroprene is widely used as refrigeration seals, motor mounts, engine coolants, petroleum and chemical tank linings, automotive seals and gasket and many others. The reason that polychloroprene is widely used is due it has a balance between its properties which make it unique among synthetic elastomers.

Some advantages of polychloroprene is as listed:

1. Good resistance mechanical strength
2. Good adhesion to many substrates
3. Good ageing resistance

2.4 Stress Softening

Mullin's effect or stress softening effect is first discovered by Mullin and Tobin in 1947. Mullin's effect generally describes a strain softening of the materials after the first loading during loading cycles. This effect is also known as the damage mechanism of a rubber material. The figure below represents occurrence of Mullin's effect under quasi-static loading. When the material is subjected to uniaxial strain, the undamaged material is stretched from 0 to an extension ratio λ_1 and the stress follows path I and the unloading follows path I' from λ_1 to 0. The second loading follows path I until $\lambda = \lambda_1$ and when $\lambda > \lambda_1$ that is λ_{II} , it follows path II. The unloading of the material from λ_2 to 0 follows path II' which is different from path I. The stress on path II is lower than path I at given stretch. The loading path when the material is stretched to λ_{III} is the path joining II and III. The unloading then follows path III'. The material will behave in an elastic manner and remains on path III' if the material is no longer stretched over the maximum stretch, λ_{III} . This behavior is referred as pseudo-elastic (Marckmann, et al,2002).

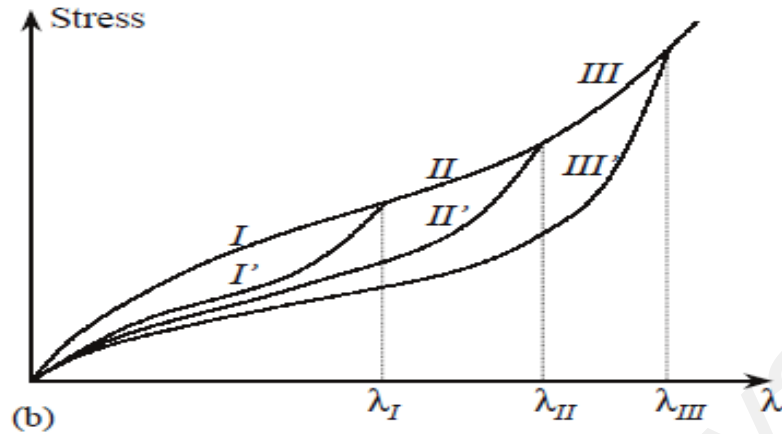


Figure 2.5: Microscopic description of Stress Softening Effect (Boyce & Qi, 2004)

During the initial loading, large hysteresis is observed. This is probably due to the dissipated strain energy caused by the rearrangement of the loading path. The extent the rubber is softened as per the Mullin effect depends on the maximum value of the strain experienced during the loading history. The larger the maximum strain experienced by the material the softer is the response (Boyce & Qi, 2004).

The reason behind the stress softening according to Mullin is the disentanglement of the network chain with the breakdown of interaction between filler particles and rubber matrix. The polymerization leads formation of chain of different length between filler particles. Two filler particles joined together by different chain is considered as illustrated in Figure 2.6. As they reach the maximum extension, the chain breaks down progressively. However another assumption was the stress softening was due to the rearrangement of the molecular network which involves displacement of network junctions.

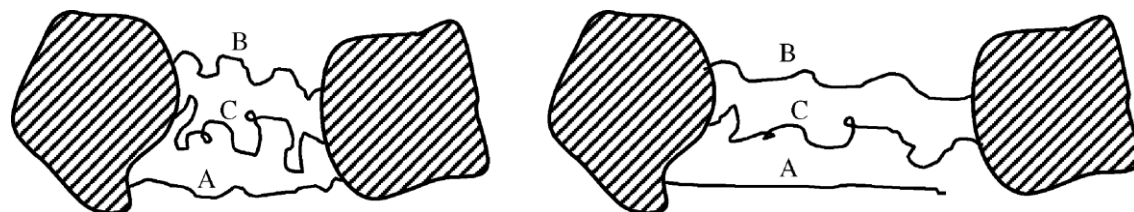


Figure 2.6: Filler particle–chain junctions (Marckmann et al, 2002)

2.5 Mechanical behavior of elastomer in biodiesel

Haseeb et al conducted a study on the compability of elastomer in palm biodiesel. The objective of the study was to investigate the degradation behavior of polychloprene, nitrile rubber and fluro viton when immersed in palm biodiesel solution (Haseeb et al, 2010). The elastomers are immersed in 100% diesel solution (B0), 10% biodiesel in diesel solution (B10) and 100% biodiesel solution (B100). After a period of time, the mass change, volume, hardness, tensile strength and elongation is measured to evaluate the degradation behavior of each material.

From the result obtained, it was observed that there was an increase of mass and volume with increasing biodiesel concentration for NBR and CR while fluro-viton did not show significant change. The swelling increase as the concentration of biodiesel increases is most probably due to the the polarization effect. Polar substance dissolves better in polar solvents and non polar substance dissolves better in non polar solvents. The positive ends of the molecules will attract the negative end of the molecules in polar solvents which is referred as

dipole-dipole interaction. In biodiesel solution, the degree of dipole-dipole interaction is higher if compared to diesel due to its additional unique chemical differences due to the increased polarity of ester. This contributes to the high swelling in biodiesel solution compared to diesel. The tensile strength, hardness and elongation of NBR and CR decreased significantly as immersed in biodiesel solution while in fluoro-viton the change is negligible. Carbon black and fillers are added to elastomer to improve hardness, abrasion and tensile strength on an elastomer which enhance cross linking between polymer chain and backbone. These cross links determine the physical properties of the elastomer. When these elastomers are exposed to biodiesel it may deteriorate the physical and mechanical properties due to the different reaction of the cross linking. More pits and cracks were observed on NBR and CR when exposed to biodiesel as compared to fluoro-viton. Also, no pits and cracks are observed in diesel. This may be due to the macromolecule chain scission or cross linking or introduction of polar oxygen groups into elastomers which would cause increase in surface energy that would lead to localized increase or decrease in density. This would promote the creation of cracks, pits and voids.

As a conclusion the study conducted significant mass and volume change in NBR and CR compared to fluoro-viton. fluoro-viton. Thus, fluoro-viton is the recommended material compared to NBR and CR to be used especially in parts in engine that will be in contact with biodiesel fuel.

Another study was conducted by Chai et al on development of a compression test device for investigation between diffusion of biodiesel and large

deformation in rubber. In this study a compressive test method was developed to observe the interaction between diffusion and large deformation in rubber (2011).

The experiment was conducted by immersing nitrile butadiene rubber (NBR) and polychloprene rubber (CR). The NBR and CR are compressed by 2%, 10% and 20 % using a special made device and then immeresed into different blend of biodiesel that is B0 (100% diesel), B25 (blend of 25 biodiesel and 75 % diesel), B75 (blend of 75 biodiesel and 25 % diesel) and B100 (100% biodiesel). Then the mass, volume, and mechanical test were conducted after 30 days and 90 days. For dry rubber, higher stress is observed compared to rubber immersed to biodiesel. As the duration of immersion increases, the stress decreases. This shows that the stress decreases with the swelling of the elastomer. This is due to the strong interaction of rubber solvent matrix system.

As a conclusion, from this study it was observed that swelling increases as the time of immersion and content of biodiesel increases. Also, less swollen material experienced higher stress compared to swollen material. An increased of mass and volume change is observed as the exposure time is increased from 30 days to 90 days for both NBR and CR. This is due more liquid are absorb until it reach a certain concentration and the liquid penetrates into the rubber by diffusion until the material reaches its equilibrium swelling. Also, the higher the concentration of biodiesel, more liquid is diffused and contributes to more swelling of the rubber. The fuel uptake is also contributed by the amount of pre-compression strain experienced by the material. The higher pre compressive strain

experienced by the material, the swelling is lesser. This is due to smaller effective area for diffusion to occur as the compressive strain is increased.

University of Malaya

CHAPTER 3: METHODOLOGY

The data for the modeling is taken from literature from Chai et al on her studies on effect of swelling on the mechanical response of elastomer under cyclic compressive loading (2011).

Several assumptions are made while performing this studies that are:

1. During mechanical loading, the volume of swollen polycholoprene remains unchanged which means the material is incompressible
2. Materials are isotropic and hyperelastic
3. Stress softening is an isotropic damage process. Thus, it could be described by scalar quantity.

As per the assumption, since the material is incompressible, the mechanical response of the material could be characterized by the existence of the strain energy density function which depends on two invariants that is I_1 and I_2 of the Cauchy-Green strain tensor \mathbf{B} and the scalar parameter d describing isotropic damage as below:

$$W = W(I_1, I_2, d) \quad (1)$$

$$\text{Where } I_1 = \text{tr}(\mathbf{B}) \text{ and } I_2 = \frac{1}{2}[I_1^2 - \text{tr}(\mathbf{B}^2)] \quad (2)$$

Following Lemaitre and Chaboche (1985), W is the strain energy of the damage material that can be considered as the product of the surface reducing parameter $1-d$ and the strain energy function of the virgin undamaged material W_0

$$W = (1 - d) \cdot W_0(I_1, I_2) \quad (3)$$

Taking the second law of thermodynamic into consideration, the Cauchy stress tensor is given by the equation below:

$$\boldsymbol{\sigma} = -p\mathbf{I} + (1 - d) \left[2\left(\frac{\partial W_0}{\partial I_1} + \frac{\partial W_0}{\partial I_2}\right)\mathbf{B} - 2\frac{\partial W_0}{\partial I_2}\mathbf{B}^2 \right] \quad (4)$$

Where $\frac{\partial W_0}{\partial I_1}$ and $\frac{\partial W_0}{\partial I_2}$ are material parameters, p is the Lagrange Multiplier and I_1 and I_2 are the first and second stress invariants respectively.

Since the effect of stress softening depends on the maximum deformation experienced by the material, therefore, a scalar measure of the deformation is required that is I_1 which is the first invariants and I_{\max} which is the maximum value of the invariant. Considering the damage parameter (d), volume rubber fraction (v_2) and principal stretch (λ) the equation below is developed:

$$d = \check{d}\left(\frac{I}{I_{\max}}, v_2\right) \quad (5)$$

$$\text{Where } I_1 = \lambda^2 + \frac{2}{\lambda} \quad (6)$$

Without losing the generalities, the focus will be on the uniaxial extension. Considering the general form of stress strain curve the fung's strain energy density function fits well. (Fung, 1967)

$$W_0 = \frac{k_1}{k_2} \exp(k_2[I_1 - 3] - 1) \quad (7)$$

Where k_1 and k_2 are material constants that are to be fitted from the first unloading curve of dry rubber that will be obtained in the next chapter.

By considering the boundary conditions to determine the Legrange multiplier, the analytical expression for the Piola-Kirchohoff stress which is engineering stress of the dry rubber (σ_{1upt}^d) is given by equation below:

$$\sigma_{1upt}^d = 2(\lambda - \frac{1}{\lambda^2})k_1 \exp(k_2(I_1 - 3)) \quad (8)$$

In order to determine the form of damage parameter, \check{d} , the stress softening (SS) and ratio stress softening (RSS) have to be considered as below:

$$SS_t^d(\frac{I}{I_{max}}) = k_5 \exp(-k_6 \frac{I}{I_{max}}) \quad (9)$$

$$RSS_t(\frac{I}{I_{max}}) = 1 - k_7 v_{2eq}(\frac{1}{v_2} - 1) \exp(-k_8 \frac{I}{I_{max}}) \quad (10)$$

Where SS_d is stress softening in dry rubber. The value of v_{2eq} is which is the rubber fraction in equilibrium swelling condition and obtained from literature. For given swelling level, by considering the two uploading curve, the below equation could be establish

$$\sigma_{2upt}^s = (1 - RSS_t^s) SS_t^d \sigma_{1upt}^s \quad (11)$$

Where σ_{1upt}^s and σ_{2upt}^s are the stresses in swollen rubber during first and second uploading respectively.

Thus in general:

$$\check{d}(\frac{I}{I_{max}}, v_2) = SS_d(\frac{I}{I_{max}}) \cdot RSS(\frac{I}{I_{max}}, v_2) \quad (12)$$

Finally the stresses during first uploading in dry and swollen rubber could be related through stress ratio star (SR^*) which is described in equation below:

$$SR_t^* \left(\frac{I}{I_{max}}, v_2 \right) = 1 - k_3 v_{2eq} \left(\frac{1}{v_2} - 1 \right) \exp \left(-k_4 \frac{I}{I_{max}} \right) \quad (13)$$

CHAPTER 4: RESULT AND DISCUSSION

The chapter is divided into three major parts. The first part will cover the development of the equations based on the experiment data. It will also cover the determination of the material parameters to fit the experiment plots and comparing the model developed with the experiment result of the first and second uploading stress for both dry and swollen rubber. The second part will cover the modeling of the deformation state using invariance. Later, the result obtained will be discussed.

4.1 Development of equations, determination of material parameters and comparisons

4.1.1 Development of equations

The damage occurs in material, d for swollen rubber is a function of strain and swelling. The strain is the maximum strain experienced by the material and is not accurate to show the stress softening effect in the swollen rubber.

The stress softening ratio of swollen rubber (SR^*) immersed in biodiesel for 30 days is calculated by dividing the first uploading stress of swollen rubber (σ_{1up}^s) with the first uploading stress of dry rubber (σ_{1up}^d) represented in the equation below:

$$SR^* = \frac{\sigma_{1up}^s}{\sigma_{1up}^d} \quad (14)$$

The value of experimental SR^* is then plotted over strain as in the following figure 4.1.

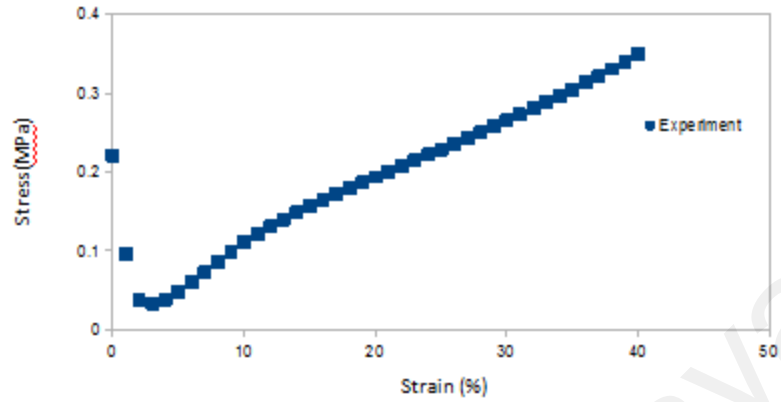


Figure 4.1: Experimental Stress Ratio

As observed from the above, the curve represents an inverse of exponential graph which could be represented as equation:

$$SR_t^* = 1 - k_3 v_{2eq} \left(\frac{1}{v_2} - 1 \right) \exp \left(-k_4 \frac{\varepsilon}{\varepsilon_{max}} \right) \quad (15)$$

Where k_3 and k_4 are the material constant that need to be identified and ε_{max} is the maximum strain applied.

As the stress ratio is a function of swelling, the swelling effect is introduced as equation below:

$$\begin{aligned}
 \text{Rubber Volume Fraction } (V_2) &= V_{\text{dry rubber}} / V_{\text{gel}} \\
 &= V_{\text{dry rubber}} / (V_{\text{dry rubber}} + V_{\text{liquid}}) \\
 &= V_{\text{dry rubber}} / V_{\text{swollen rubber}} \\
 &= V_o / V_i \quad (16)
 \end{aligned}$$

We can now define swelling, β as a function of a rubber volume fraction:-

$$\begin{aligned}
 \text{Swelling } (\beta) &= (V_i - V_o)/V_o \\
 &= (V_i/V_o) - 1 \\
 &= (1/V_2) - 1
 \end{aligned} \tag{17}$$

Where, V_{2eq} is the highest value of swelling for the material (equilibrium condition). The value of V_{2eq} for polychloroprene (CR) is 0.42. Consider the stress ratio (SR^*) as follow:

$$SR^* = 1 - f(\epsilon) \tag{18}$$

Where,

$$f(\epsilon) = k_3 V_{2eq} (1/V_2 - 1) \exp(-k_4 \epsilon/\epsilon_{max}) \tag{19}$$

If $V_2 = 1$, then $f(\epsilon) = 0$ which represent the condition for dry rubber and if $V_{2eq} < V_2 < 1$ then $f(\epsilon) > 0$ which represent condition for the swollen rubber.

The next equation that needs to be developed is the stress softening equation for dry rubber (SS_d) is derived in order to develop a modeling of second uploading stress for swollen rubber. It is calculated by dividing the difference between first and second uploading stress with the first uploading stress as represented in equation below:

$$SS^d = \frac{\sigma_{1up}^d - \sigma_{2up}^d}{\sigma_{1up}^d} \tag{20}$$

From the experiment value plotted, it is observed that the stress softening for dry rubber is decreasing exponentially. Since the stress softening represents dry rubber, the effect of swelling is ignored. The equation below is developed to represent the curve in Figure 4.2.

$$SS_t^d = k_5 \exp \left(-k_6 \frac{\varepsilon}{\varepsilon_{max}} \right) \quad (21)$$

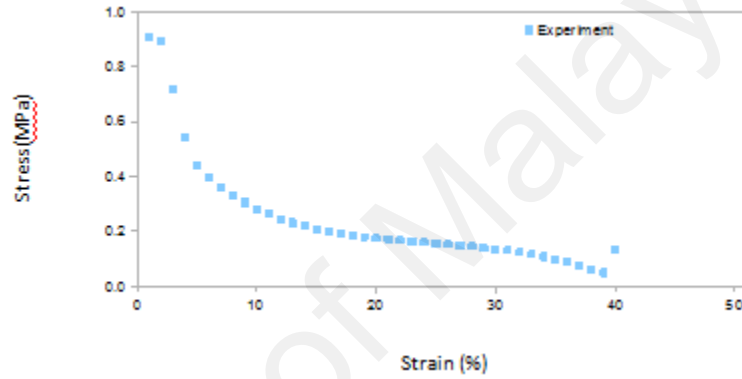


Figure 4.2: Experimental Stress Softening for dry rubber

Where k_5 and k_6 is a material constant that need to be identified so that the experiment value will be as close as the developed model.

Next for the ratio of stress softening (RSS) where the value is obtained from dividing the stress softening of swollen material (SS^s) to the value of stress softening of dry material (SS^d) as below:

$$RSS^s = \frac{SS^s}{SS^d} \quad (22)$$

The figure 4.3 show the experiment RSS plotted against strain for dry and rubber immersed in biodiesel for 30 days.

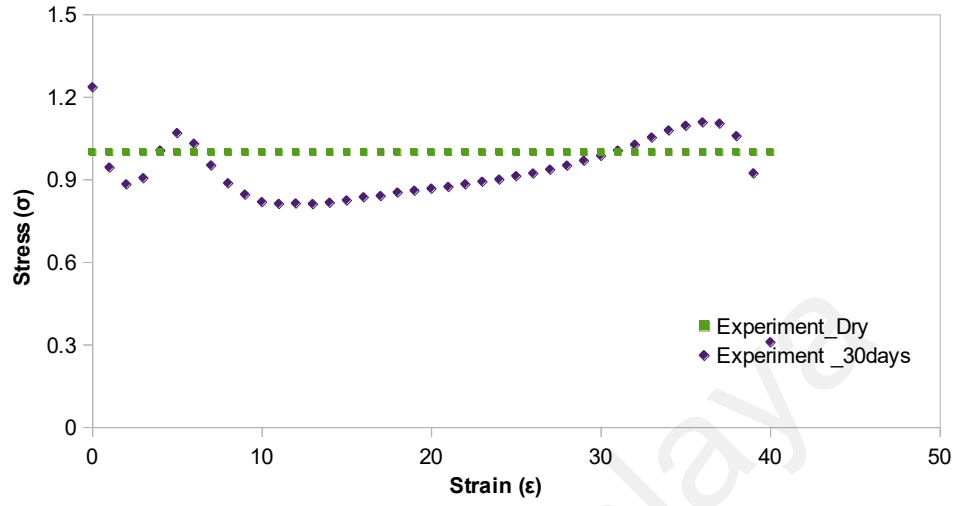


Figure 4.3: Experimental Ratio of Stress Softening

From the graph, we can observe that, the RSS curve is similar to the stress ratio (SR^*) curve which is in inverse exponential shape. Since RSS equation is developed for swollen rubber, the effect of swelling must be considered. Therefore, we propose the same model as SR^*

$$RSS_t = 1 - k_7 v_{2eq} \left(\frac{1}{v_2} - 1 \right) \exp \left(-k_8 \frac{\epsilon}{\epsilon_{max}} \right) \quad (23)$$

Where k_7 and k_8 are material constants obtained by fitting the experimental with the theoretical plot.

4.1.2 Material constant determination

After the equations from the experimental value are obtained, the material constants need to be obtained by fitting the experimental data with the equations developed.

From the Fung strain energy density function as in Equation 7, the experimental curve for the stress at the first uploading of dry rubber is plotted along the theoretical model proposed as per equation 8. The value of k_1 obtained is 0.9MPa and the value of k_2 is 0.001

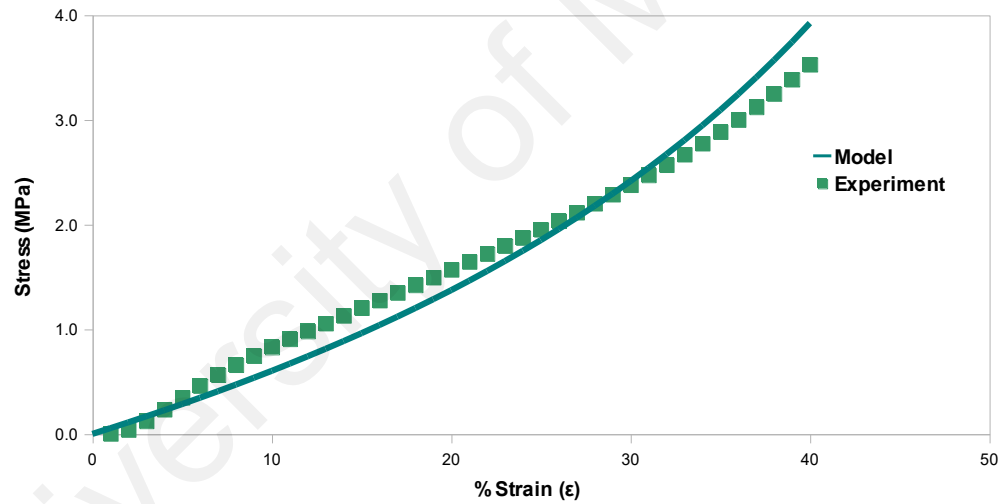


Figure 4.4: Stress at first uploading for dry rubber

For the stress ratio (SR^*), the plot of the model versus the experiment is plotted as figure 4.5 below and the value obtained for k_3 is 2.0 and k_4 is 0.4

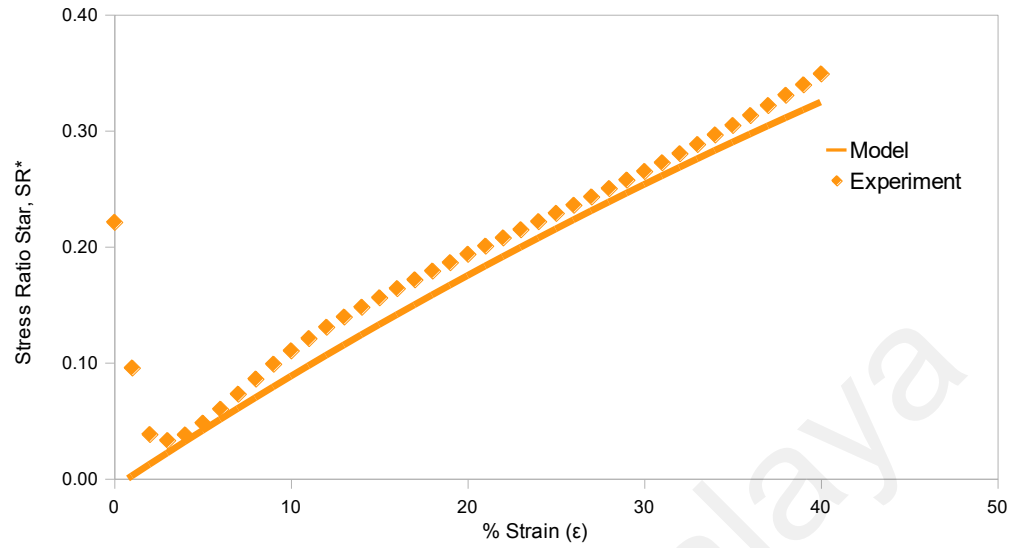


Figure 4.5: Stress Ratio of experimental and model

In order to obtain the value of k_5 and k_6 from the stress softening model proposed as in Equation 21, the theoretical and experimental graph is plotted as in figure 4.6 and the value of k_5 and k_6 obtained is 0.45 and 1.8 respectively.

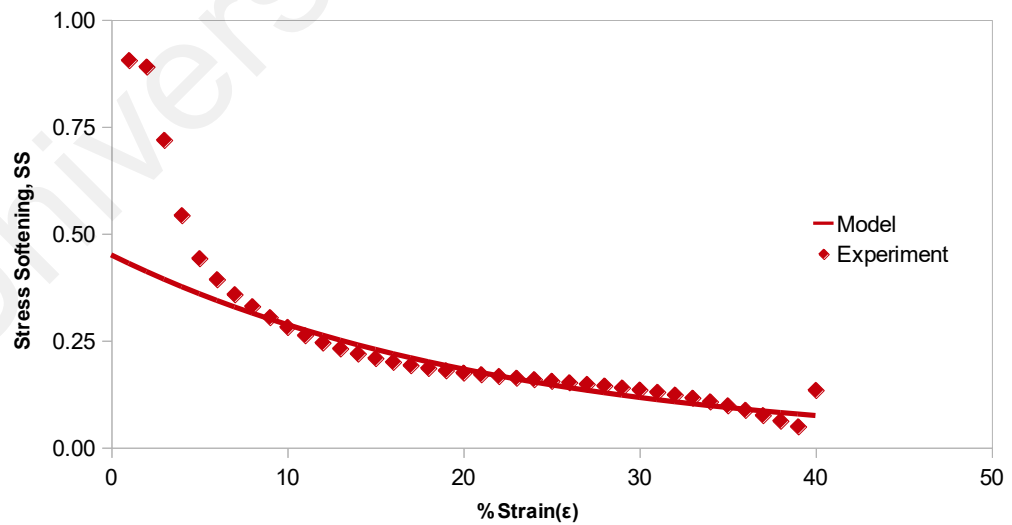


Figure 4.6: Experimental and theoretical stress softening curve for the dry rubber

To obtain the value of k_7 and k_8 from the stress softening equation proposed as in equation 23, the theoretical and experimental graph is plotted as in figure 4.6 and the value of k_7 and k_8 obtained is 2.5 and 5.0 respectively

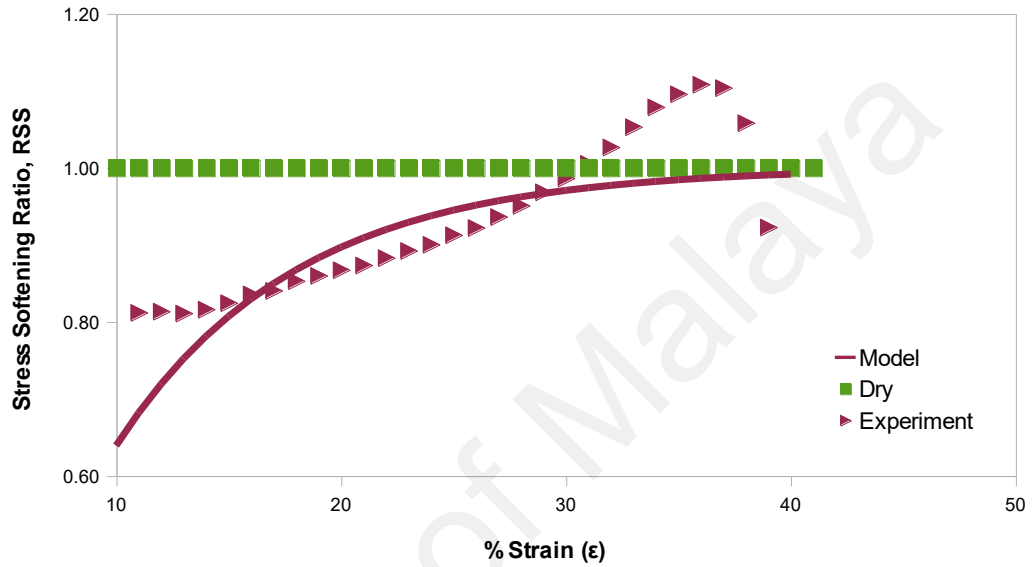


Figure 4.7: The experimental and theoretical curve for ratio of the stress softening

The value of all the material constants from k_1 to k_8 is summarized in table 4.1 below:

Table 4.1: The value of material constant

k_1	k_2	k_3	k_4	k_5	k_6	k_7	k_8
0.9MPa	0.001	2.0	0.4	0.45	1.8	2.5	5.0

4.1.3 Comparison model with experimental result

With all the value of material parameters, k obtained the theoretical stress of first and second uploading for dry and swollen rubber is plotted and compared with experiment result. For the first uploading stress for dry rubber, equation as given in Equation 8 is used while for swollen rubber, the equation below is used.

$$\sigma_{1upt}^s = \sigma_{1upt}^d SR * \quad (24)$$

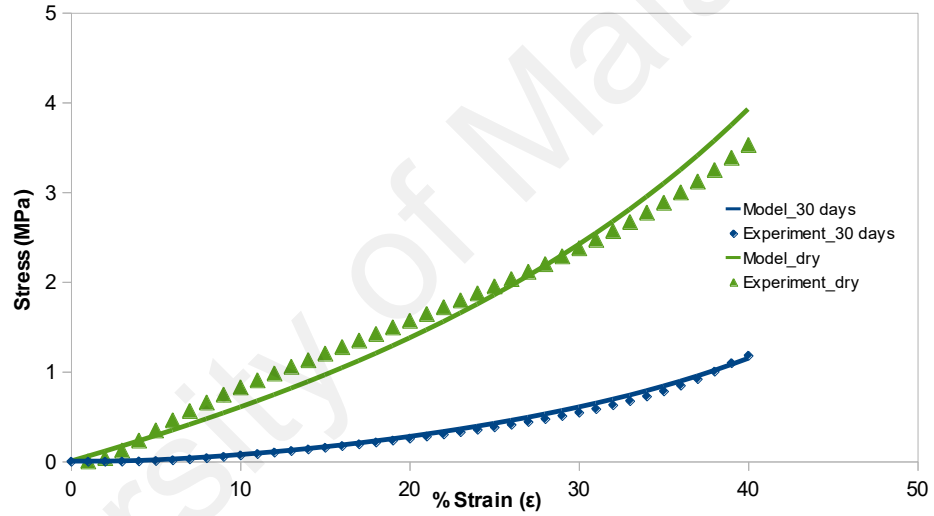


Figure 4.8: Stress at first uploading

The second uploading stress for both dry and swollen are plotted as in figure 4.9. Equations 25 and 26 are used model the value of second uploading stress for dry and swollen respectively.

$$\sigma_{2upt}^d = (1 - SS)\sigma_{1upt}^d \quad (25)$$

$$\sigma_{2upt}^s = (1 - RSS_t^s)SS_t^d\sigma_{1upt}^s \quad (26)$$

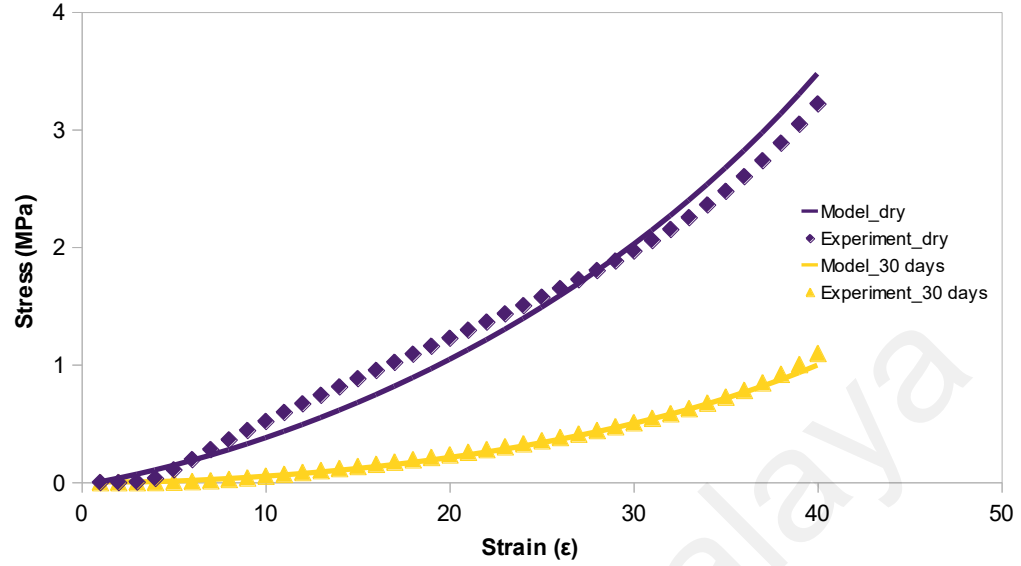


Figure 4.9: Stress at second uploading

From figure 4.8 and 4.9, we can now conclude that the equation models developed gives a qualitatively good agreement with the experiment.

4.2 Modeling with the Stress Invariants

The second part is plotting all the above stress invariants. The methods are similar as used in the previous sections. The modification done is the theoretical graph is plotted as a function of I_1 which means the ϵ/ϵ_{\max} is replaced with I/I_{\max} .

The first uploading stress using the 8 chain model is similar as in Figure 4.4 and the value of k'_1 and k'_2 obtained from this curves is 0.9 and 0.001. This value does not differ as in Equation 8 as the equation does not have the function ϵ/ϵ_{\max} that is replaced with I/I_{\max} .

Figure 4.10 shows the stress ratio graph which developed from a modification of equation 15 and is as below. The value of k'_3 and k'_4 obtained is 4.4 and 1.2.

$$SR_t^* = 1 - k_3 v_{2eq} \left(\frac{1}{v_2} - 1 \right) \exp \left(-k_4 \frac{\varepsilon}{\varepsilon_{max}} \right) \quad (27)$$

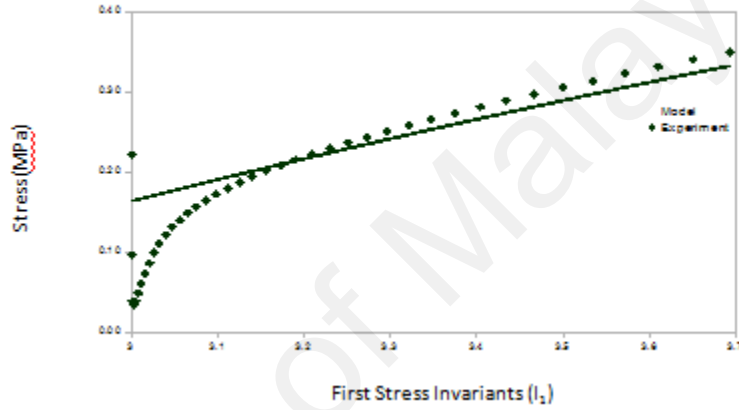


Figure 4.10: Stress Ratio as a function of I_1

In figure 4.11, the stress softening graph is plotted by using a modification of equation 21 and compared with the experimental. The value of k'_5 and k'_6 obtained is 0.45 and 1.2. The equation is re-written as:

$$SS_t^d = k'_5 v_{2eq} \left(\frac{1}{v_2} - 1 \right) \exp \left(-k'_6 \frac{I}{I_{max}} \right) \quad (28)$$

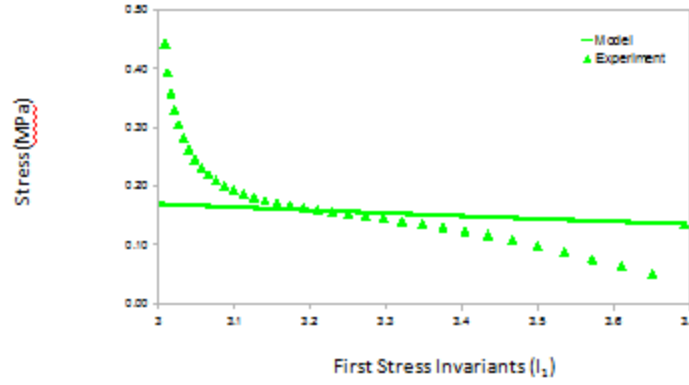


Figure 4.11: Stress Softening as a function of I_1

The theoretical ratio of stress softening graph for CR is then plotted by using a modification of equation 23 as is represented as in figure 4.12. The material constant k'_7 obtained is and k'_8 is 2.5 and 4.0. The equation is written as below:

$$RSS_t = 1 - k'_7 v_{2eq} \left(\frac{1}{v_2} - 1 \right) \exp \left(-k'_8 \frac{I}{I_{max}} \right) \quad (29)$$

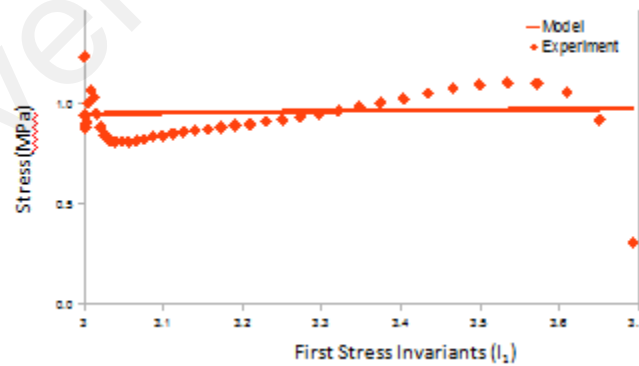


Figure 4.12: Stress Softening as a function of I_1

The summary of all constant value is shown in table 4.2.

Table 4.2: Summary of material constant value in 8-chain model

k'_1	k'_2	k'_3	k'_4	k'_5	k'_6	k'_7	k'_8
0.9MPa	0.001	4.4	1.2	0.45	1.2	2.5	4.0

By using all value of material constant, k obtained the stress at first and second uploading as a function of I_1 is plotted as shown in figure 4.14 and 4.15. It is shown that from the figure, the experimental and theoretical curve showing the good agreement with each other.

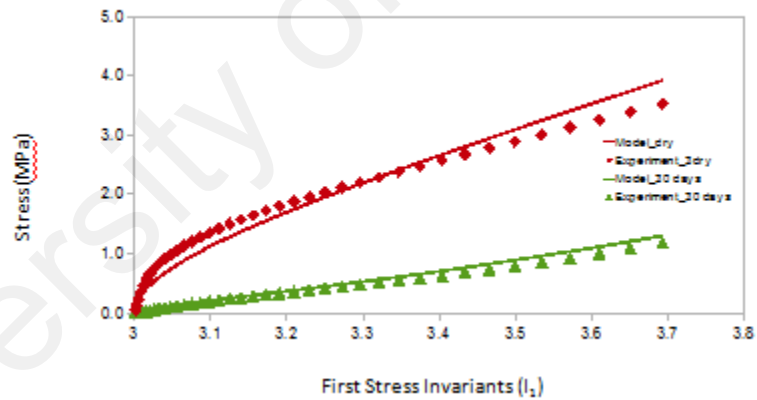


Figure 4.13: Stress at first uploading as a function of I_1

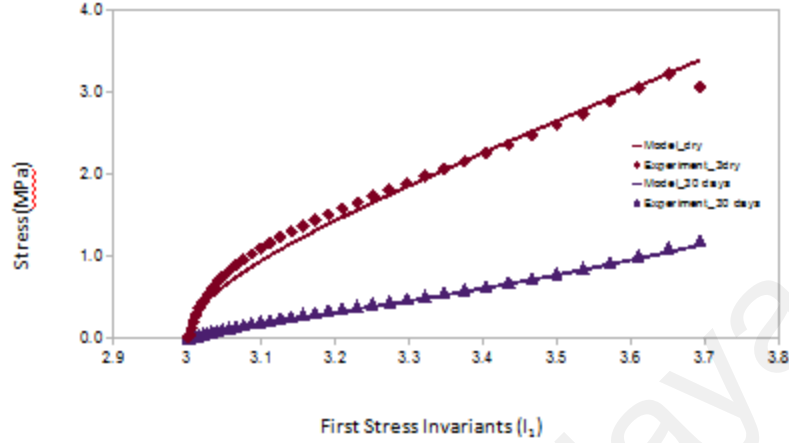


Figure 4.14: Stress at second uploading as a function of I_1

4.3 Discussion

It had been shown from figure 4.8 and 4.9; the theoretical model qualitatively agrees with the experimental. A good agreement of the model equation developed with the experiment result is observed for the swollen rubber. The curve for the dry rubber fits well in lower and higher stress but deviates a little bit in the middle part.

It is discovered that determination of the material parameters k_1 and k_2 determined from equation 8 plays an important role and effects largely the subsequent uploading stresses. Thus, the choice of the right strain energy density function plays a vital role. Hence it could be concluded that Fung's Strain energy density function seems to be appropriate for this study

Both stress at first and the second uploading from theoretical model is then plotted as in figure 4.15.

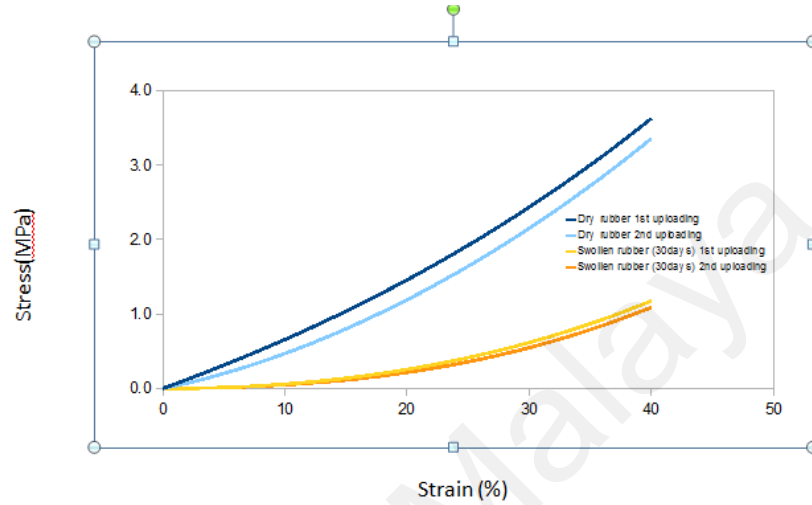


Figure 4.15: Theoretical stress at first and second uploading

From the observation in Figure 4.15, it is observed that swollen rubber has lower stress compared to dry CR with the same strain rate. Also, the first uploading stress differs from the second uploading stress for both swollen and dry CR. This means that the CR material exhibits stress softening.

The plot captured using the 8-chain model also shows a good agreement between the experimental and developed model as illustrated in figure 4.13 and 4.14. From these observations it could be agreed that the models developed in this study qualitatively agree.

From the stress softening equation as in Equation 20, the graph for stress softening in swollen rubber is plotted as in figure 4.16 and compared with dry

rubber. It is observed from the graph, the stress softening value which represents the damage mechanism is lower in swollen rubber compared with dry rubber at a given strain.

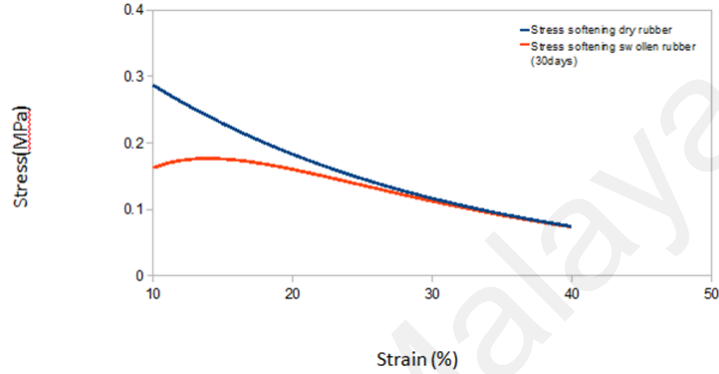


Figure 4.16: Stress softening of swollen rubber compared to dry rubber

The CDM model by Chagnon et al, 2004 showing in Equation 1 is a damage phenomenon which the strain energy is referred by scalar quantity of damage parameter, d . In swollen rubber, d is a function of strain and swelling.

By adopting the Kachanov type of equation which proposed by Simo, quoted by Diani et al (2006), the damage parameter is refer to the different path of uploading stress. The following equation is used to see the relationship between the Mullin effect and damage phenomenon:

$$\sigma^{2up} = (1 - d) \sigma^{1up} \quad (30)$$

Then,

$$(1 - d) = \sigma^{2up} / \sigma^{1up} \quad (31)$$

Stress ratio is defined as:

$$\text{Stress Ratio} = \sigma^{2\text{up}} / \sigma^{1\text{up}} \quad (32)$$

Thus;

$$(1 - d) = \text{Stress Ratio} \quad (33)$$

Damage material can be defined as a stress softening by following:

$$\begin{aligned} \text{Stress Softening (SS)} &= (\sigma^{1\text{up}} - \sigma^{2\text{up}}) / \sigma^{1\text{up}} \\ &= 1 - (\sigma^{2\text{up}} / \sigma^{1\text{up}}) \\ &= 1 - \text{Stress Ratio} \\ &= 1 - (1 - d) \end{aligned} \quad (34)$$

We can now define d as:

$$\begin{aligned} 1 - d &= 1 - \text{SS} \\ d &= \text{SS} \end{aligned} \quad (35)$$

From the above derivation it can be concluded that the damage phenomenon in this model is a stress softening phenomenon. If value of $d = 0$, there is no damage which mean there is no stress softening in the material.

CHAPTER 5: CONCLUSION AND RECOMMENDATIONS

5.1 Conclusion

A simple continuum mechanical model was developed to capture stress softening effect in swollen rubber under cyclic loading. The data of the experiment was taken from literature where a study is done on effect of swelling on the mechanical response of elastomer under cyclic compressive loading. Then experiment data were plotted from the result obtained and some simple equation. From the experimental data, mathematical model were developed to represent the data. The mathematical model was fit to the experiment result by material parameters from k_1 to k_8 . From the plot above, it could be observe that as the strain reaches its maximum value the stress softening appears to be decreasing. From the plot it is observed that the more swelling experienced by the material the stress softening is decreased as the material approaches its maximum strain value. However, there are some discrepancies observed in the low comparative strain. This may be attributed to the fact that the stress is too low at low comparative strain that the proposed equation to define stress softening is unable to show its best stress softening value. Besides that lower stress softening is value is observed with more swelling most probably due to strong rubber solvent interaction

5.2 Recommendations

There are few recommendations that could be considered in order to study more the effect of stress softening effect in elastomer under cyclic loading as listed below:

1. A simple and better equation could be developed for plotting the experimental value of stress softening.
2. To verify with further experiment whether the material is incompressible as per assumption
3. To develop a model by taking into material compressability.
4. To compare the swelling of a few material besides polychloroprene under cyclic loading

BIBLIOGRAPHY

Background: Biodiesels and Other Biofuels. (2008, June 18). Retrieved April 27, 2012, from <http://www.nora-oilheat.org/site20/uploads/factfinding1>

Basiron, Y. (2007). Palm oil production through sustainable plantations. *Eur. J. Lipid Sci. Technol.* 109 , 289-295.

Bauman, J. T. (2006). Rubber Stress-Strain Behavior. In J. T. Bauman, *Fatigue, Stress, and Strain of Rubber Components* (pp. 9-18). Hanser.

Boyce, M., & Qi, H. (2004). Constitutive model for stretch-induced softening of the stress–stretch behavior of elastomeric materials. *Journal of the Mechanics and Physics of Solids* .

Chai, A., Andriyana, A., Verron, E., Johan, M., & Haseeb, A. (2011). Development of Compression Test Device for Investigating Interaction between Diffusion of Biodiesel and Large Deformation in Rubber. *Polymer Testing* , 867-875.

Crimson Renewable Energy. (2007). Retrieved April 27, 2012, from Crimson Renewable Energy: www.crimsonrenewable.com

Demirbas, A. (2008). Biofuels sources, biofuel policy, biofuel economy and global biofuel projections. *Energy Conversion and Management* 49 , 2106–2116.

Demirbas, A. (2009). Progress and recent trends in biodiesel fuels. *Energy Conversion and Management* , 14-34.

Elastomer Properties. (n.d.). Retrieved April 27, 2012, from Elastomer Properties: www.stoeffl.com

Geiver, L. (2011, May 27). *Biodiesel Magazine*. Retrieved April 27, 2012, from Biodiesel Magazine: <http://www.biodieselmagazine.com/issues/browse/>

Gerpen, J. V. (2006). Biodiesel Production and Fuel Quality. 1-24.

Hansen, A. C., Qin, Z., & Robert, H. H. (2009). *Engine Fuel System Durability*. University of Illinois,.

Haseeb, A., Masjuki, H., Siang, C., & Fazal, M. (2010). Compatibility of Elastomer in Palm Biodiesel. *Renewable Energy* , 2356-2361.

Howell, S., & J., A. W. (n.d.). *Biodiesel Use in Underground Metal and Non-metal Mines*. Retrieved April 27, 2012, from Biodiesel Use in Underground Metal and Non-metal Mines: <http://www.dieselnet.com/papers/9705howell.html>

Karl, T. L. (2007). Oil-Led Development: Social, Political, and Economic Consequences. *CDDRL WORKING PAPERS* , 23-56.

Kerwin, J. (2007, June 23). Biofuels Put Seals to the Test. Greenbank Road, London, United Kingdom.

Marckmann, G., Verron, E., Gorneta, J. L., Chagnon, G., Charrier, P., & Fort, P. (2002). A theory of network alteration for the Mullins effect. *Journal of the Mechanics and Physics of Solids* , 2011 – 2028.

MN, I., & Beg, M. (2004). The fuel properties of pyrolysis liquid derived from urban solid wastes in Bangladesh. *Bioresour Techno* , 181-187.

Mohammed, M. (2011). *Mathematical Modeling of a Two-Phase Bubble-Column Reactor for*. Philadelphia: Drexel University.

Shigeaki, H., Hideo, K., Yuki, K., & Kazuaki, S. (1999). Petroleum Biodegradation in Marine Environments. *J. Molec. Microbiol. Biotechnol* , 63-7